

## Magnetic and martensitic phase transitions in ferromagnetic Ni-Ga-Fe shape memory alloys

著者	及川 勝成
journal or publication title	Applied Physics Letters
volume	81
number	27
page range	5201-5203
year	2002
URL	<a href="http://hdl.handle.net/10097/34928">http://hdl.handle.net/10097/34928</a>

# Magnetic and martensitic phase transitions in ferromagnetic Ni–Ga–Fe shape memory alloys

K. Oikawa<sup>a)</sup>

National Institute of Advanced Industrial Science and Technology, Tohoku Center, Sendai 983-8551, Japan

T. Ota, T. Ohmori, Y. Tanaka, H. Morito, A. Fujita, R. Kainuma, K. Fukamichi,  
and K. Ishida

Department of Materials Science, Graduate School of Engineering, Tohoku University,  
Sendai 980-8579, Japan

(Received 5 August 2002; accepted 28 October 2002)

Ferromagnetic shape memory alloys with a body-centered-cubic ordered structure in a Ni–Ga–Fe system have been developed. The alloys with the composition range of Ni 27 at. % Ga (20–22 at. %)Fe exhibit a thermoelastic martensitic transformation from a B2 and/or an L2<sub>1</sub> parent to a martensite phase, with a seven-layer modulated (14M) and a five-layer modulated (10M) structure, in the ferromagnetic state. The parent phase transforms from the B2 to the L2<sub>1</sub> structure at about 970 K during cooling, and the degree of the L2<sub>1</sub> order in the parent phase is increased by annealing at 773 K, resulting in the increase of both the martensite starting and the Curie temperatures. The ductility of these alloys is improved by introducing of a small amount of a  $\gamma$ -phase solid solution. Consequently, we can conclude that the present alloys are promising for ferromagnetic shape memory alloys. © 2002 American Institute of Physics. [DOI: 10.1063/1.1532105]

Ferromagnetic shape memory alloys (FSMAs) have received much attention as high performance magnetically controlled actuator materials, because they show a large magnetic-field-induced strain by the rearrangement of twin variants in the martensite phase. Until now, several candidates for FSMAs have been reported including Ni<sub>2</sub>MnGa,<sup>1,2</sup> Fe–Pd,<sup>3</sup> Fe–Pt,<sup>4</sup> Ni<sub>2</sub>MnAl,<sup>5,6</sup> and Co<sub>2</sub>NiGa<sup>7</sup> systems. Recently, the present authors have found promising FSMAs in Co–Ni–Al and Co–Ni–Ga  $\beta$  [B2 ordered body-centered-cubic (bcc) structure]-based alloys.<sup>8–10</sup> These alloys are characterized by a wide range of the transition temperature from 120 to 420 K and excellent ductility. A large magnetic-field-induced reversible strain of about 600 ppm was confirmed in the martensite phase of the Co–Ni–Al  $\beta$  single crystal<sup>11</sup>

Co–Ni–(Al and Ga) ternary systems with the  $\beta$  phase exist over a wide range of composition. The ferromagnetism of these alloys may be closely correlated with Co antistructure atoms on the Al or Ga sites in the B2 structure. Since the B2 phase appears in both the Fe–Ga and Ni–Ga binary systems,<sup>12</sup> the solid solution of the B2 phase may also be formed in the wide range of composition in the Ni–Ga–Fe ternary system. Accordingly, it is expected that ferromagnetism due to Fe antistructure atoms on the Ga site can be obtained in some B2 phase region alloys. Furthermore, the thermoelastic martensite transformation from the B2 to the tetragonal phase is expected in the Ni-rich side of the Ni–Ga–Fe system in analogy with the Co–Ni–Ga  $\beta$  alloys.<sup>7,9</sup> The atomic and magnetic orderings and the martensitic transformations in the Ni–Ga–Fe B2 phase alloys, however, have not been reported yet. In the present study, these transitions in the B2 phase alloys have been investigated, and revealed that the atomic ordering from the B2 to the L2<sub>1</sub> structure and

the martensitic transformation from the L2<sub>1</sub> to the modulated layer (14M and/or 10M) structure associated with a shape memory effect take place in the ferromagnetic state.

Ni<sub>73-x</sub>Ga<sub>27</sub>Fe<sub>x</sub> alloys ingots ( $x$  is from 19 to 25 at. %), weighing about 20 g each were prepared by melting pure iron, nickel, and gallium in a cold crucible levitation melting furnace under an argon gas atmosphere, and were cast into a copper mold. The small specimens were taken from the ingots and sealed in a quartz capsule filled with argon gas for heat treatment. The samples were heat treated at 1473 K for 3 h to prepare homogeneous single phase alloys and were quenched into ice water. After quenching, some selected samples were heat treated at 773 K for 1 h to promote the atomic ordering in the parent phase and then quenched into ice water. The magnetic properties were measured with a vibrating sample magnetometer, and the martensitic transformation temperatures  $M_s$  and  $A_f$  were determined by differential scanning calorimetry in cooling and heating processes at a rate of 10 K/min. The Curie temperature  $T_C$  was defined as the minimum point of the temperature derivative of magnetization ( $dM/dT$ ) versus temperature ( $T$ ), under field strength  $H$  of 500 Oe. Transmission electron microscopic (TEM) observation below room temperature was conducted to identify the crystal structure of both the parent and martensite phases.

In Fig. 1, the Curie temperature  $T_C$ , the martensitic transformation starting temperature  $M_s$ , and the reverse transformation finishing temperature  $A_f$  are plotted as a function of Fe content in the 27 at. % Ga section. The values of  $M_s$  and  $A_f$  decrease and  $T_C$  increases with increasing Fe content. All these characteristic temperatures of the samples annealed at 773 K are higher than those annealed at 1473 K. Since the transformation temperature hysteresis ( $A_f - M_s$ ) is 15 K or less, the transformation mode is considered as a thermoelastic type. The value of  $T_C$  is higher than  $M_s$  and  $A_f$

<sup>a)</sup>Electronic mail: k-oikawa@aist.go.jp

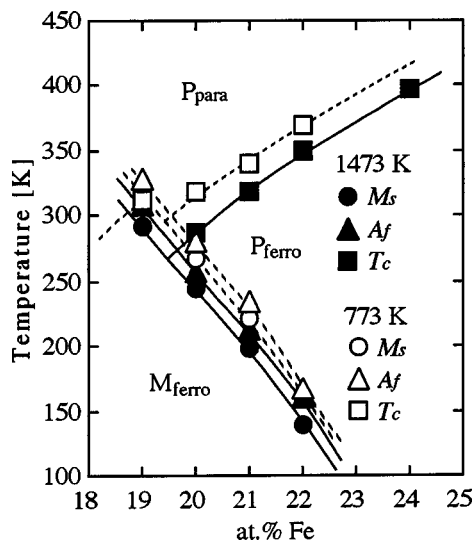


FIG. 1. Composition dependence of  $T_c$ ,  $M_s$ , and  $A_f$  in  $\text{Ni}_{73-x}\text{Fe}_x\text{Ga}_{27}$  annealed at 1473 and 773 K. The parent and the martensite phases are given by P and M, respectively.

in the alloys with the Fe composition above 20 at. %, indicating that these alloys are FSMAs.

The TEM bright-field image and the corresponding selected area diffraction (SAD) pattern at 90 K for the  $\text{Ni}_{51}\text{Ga}_{27}\text{Fe}_{22}$  alloy annealed at 773 K are shown in Fig. 2. A typical morphology of the modulated layer structure with a high twin density is observed and the  $x/5\{220\}L_{21}$  extra spots characterized as the 10M structure<sup>13</sup> are detected. A similar twin structure is observed at 90 K in the same alloy annealed at 1473 K. However, the corresponding SAD pattern exhibits the  $x/7\{220\}L_{21}$  extra spots defined as the 14M structure.<sup>13</sup> The same structures were confirmed in the other alloys. Figure 3(a) shows the SAD pattern at room temperature for the  $\text{Ni}_{51}\text{Ga}_{27}\text{Fe}_{22}$  alloy annealed at 773 K. The  $\{111\}L_{21}$  extra spots characterized as the  $L_{21}$  are observed. The dark-field image (DFI) taken from the  $\{111\}L_{21}$  reflection of the alloy quenched from 1473 K shows the small antiphase domains (APDs) with 10–30 nm in diameter as given in Fig. 3(b), while no APD structure is observed in the same specimen from the  $\{200\}L_{21}$  reflection defined as the B2 structure. This fact implies that the parent phase has the B2 structure at 1473 K and the atomic ordering from the B2 to the  $L_{21}$  structure follows during quenching. The DFI taken from the  $\{111\}L_{21}$  reflection of the  $\text{Ni}_{51}\text{Ga}_{27}\text{Fe}_{22}$  alloy

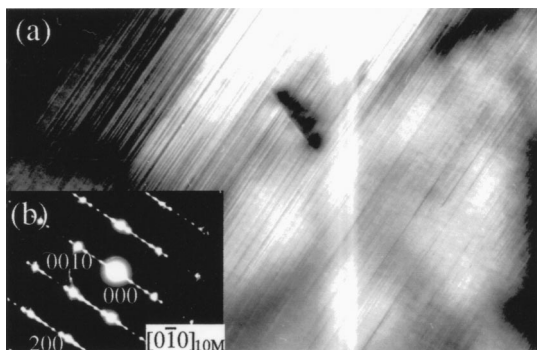


FIG. 2. (a) TEM bright-field image showing the typical microstructure and (b) the corresponding SAD pattern at 90 K taken from the martensite phase of  $\text{Ni}_{51}\text{Fe}_{22}\text{Ga}_{27}$  alloy annealed at 773 K.

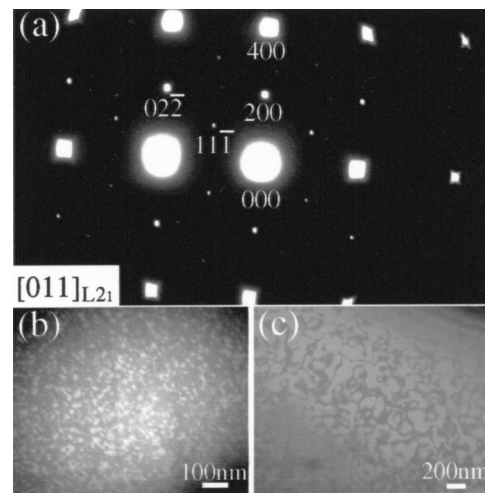


FIG. 3. (a) SAD pattern obtained from the alloy annealed at 773 K and TEM DFIs taken from  $\{111\}L_{21}$  reflection of the parent phase in  $\text{Ni}_{51}\text{Fe}_{22}\text{Ga}_{27}$  alloy annealed at (b) 1473 and (c) 773 K.

annealed at 773 K is shown in Fig. 3(c). The APDs grew up during the annealing. The B2/ $L_{21}$  ordering temperature was confirmed to be about 970 K by the DSC measurement.

The thermomagnetization ( $M-T$ ) curves of the  $\text{Ni}_{51}\text{Ga}_{27}\text{Fe}_{22}$  alloys annealed at 773 and 1473 K are shown in Fig. 4. For the specimen annealed at 773 K, the magnetization at  $A_f$  in the magnetic field of 1 kOe increases and that in 15 kOe decreases as seen from Fig. 4(a). The increase of the magnetization at  $A_f$  during heating was preferably observed at lower magnetic fields. These characteristic features are similar to those of other FSMAs.<sup>8,14</sup> Thus, the magnetization ( $M-H$ ) curve of the parent phase is more easily saturated than that of the martensite phase, because the martensite phase has higher magnetocrystalline anisotropy energy (MAE) than the parent phase. On the other hand, the  $M-T$

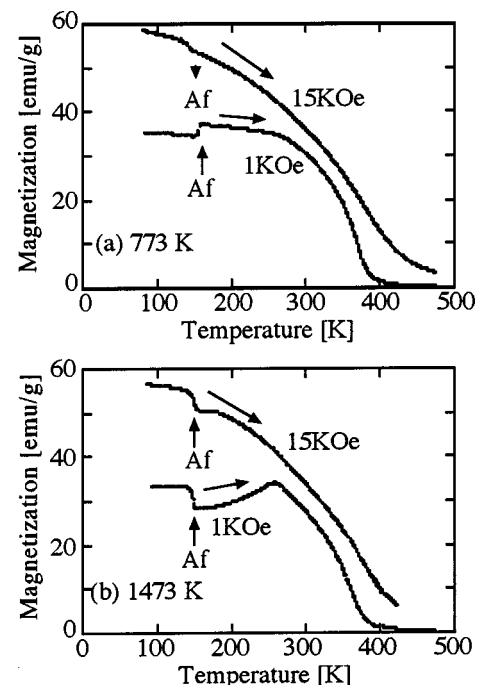


FIG. 4. Thermomagnetization curves in the magnetic fields of 1 and 15 kOe for  $\text{Ni}_{51}\text{Fe}_{22}\text{Ga}_{27}$  alloy annealed at (a) 773 K and (b) 1473 K.

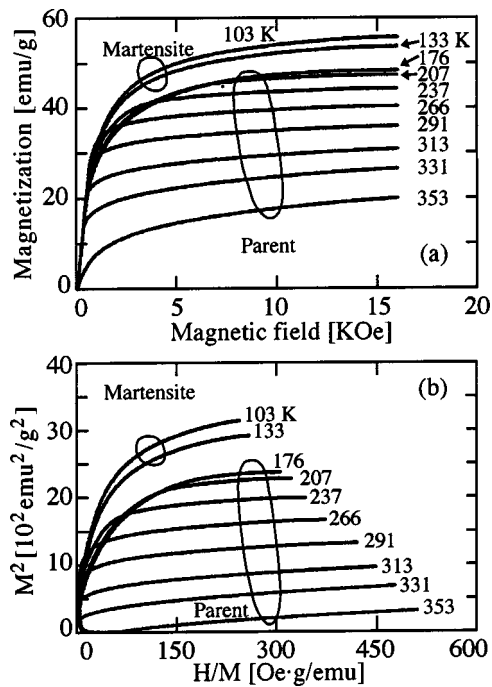


FIG. 5. Magnetic properties of  $\text{Ni}_{51}\text{Fe}_{22}\text{Ga}_{27}$  alloy annealed at 1473 K. (a) Magnetization curves and (b) Arrott plots at various temperatures.

curves for the specimen annealed at 1473 K in 1 and 15 kOe decrease at  $A_f$  as shown in Fig. 4(b). The decrease of the magnetization was observed even in much lower magnetic fields, which is opposite to the trend of other FSMAs. The  $M-H$  curves at various temperatures on the heating process for the  $\text{Ni}_{51}\text{Ga}_{27}\text{Fe}_{22}$  alloy annealed at 1473 K are shown in Fig. 5(a). In Fig. 5(a), the demagnetizing field was corrected. The magnetization curves of the parent phase are not saturated above  $A_f$  even at the magnetic field of 15 kOe. Figure 5(b) shows the Arrott plots for the data in Fig. 5(a). The plots in the parent phase higher than 207 K show a straight line at high magnetic fields, while the plots at 176 K just above  $A_f$  exhibit strong convex curves upwards. An electrical resistivity measurement was made to verify that no intermediate phase transition as reported in the  $\text{Ni}_2\text{MnGa}$  occurred. Therefore, this result may be closely correlated with the pinning effect of the nanoscale APDs shown in Fig. 3(b) on magnetic domain-wall migration. However, the features of the Arrott plots are very sensitive to magnetic states in specimens and, hence, further investigations are necessary for a detailed discussion on the relation between the magnetic properties and the APDs. The saturation magnetization  $M_s$  and the high-field susceptibility  $\chi_{hf}$  of the martensite phase at 103 K are estimated from the law of approach to saturation given by

$$M = M_s(1 - a/H - b/H^2) + \chi_{hf}H, \quad (1)$$

where  $a$  and  $b$  are the fitting coefficients.  $M_s$  and  $\chi_{hf}$  were evaluated as 51.9 emu/g and 0.0003 emu/g/Oe, respectively. The coefficient  $b$  was evaluated as 157 800 emu·Oe<sup>2</sup>/g, implying that the MAE of the martensite phase is large.

The thermally induced shape memory properties in the ferromagnetic state were examined by the bending test. The

single-phase polycrystalline alloys are very brittle. On the other hand, the point to notice is that the composition range of the  $L_{21}$  phase showing the FSM is located near the  $L_{21} + \gamma$  (face-centered-cubic Al structure) two-phase region. Thus, a small amount of the  $\gamma$ -phase can be introduced into the  $L_{21}$ -based FSMAs which brings about a drastic improvement of ductility through the same way as in the Co–Ni–Al FSMAs.<sup>8</sup> The  $\text{Ni}_{53}\text{Ga}_{26.5}\text{Fe}_{20.5}$   $L_{21} + \gamma$  two-phase specimens with 200  $\mu\text{m}$  thick were prepared by hot rolling at 1373 K and subsequent cold rolling. The  $\gamma$ -phase fraction of precipitated was evaluated to be about 4%. The values of  $M_s$ ,  $A_f$ , and  $T_C$  are 234, 249, and 318 K, respectively. The thin plates were bent to realize a surface strain of 2% at 90 K. Upon heating above  $A_f$  to 423 K, the shape recovery of about 90% was obtained. Since the martensite phase is considered to have a large MAE and the variant boundaries of the martensite phase such as 10M and 14M are considered to have a high mobility,<sup>15</sup> it is expected that a large magnetic-field-induced strain could be obtained in this alloy system. Details of these results will be reported in the near future.

In conclusion, Ni–Ga–Fe FSMAs have been developed. The alloys with the composition range Ni 27 at.% Ga (20–22 at.%)Fe exhibit a thermoelastic martensitic transformation in the ferromagnetic state associated with a shape memory effect. The parent phase transforms from a B2 to a higher ordered  $L_{21}$  structure at about 970 K during cooling. The parent phases martensitically transform to a 10M and/or a 14M modulated layer structures in the samples annealed at 773 and 1473 K. Annealing at 773 K promotes the  $L_{21}$  ordering of the parent phase and increases both the martensitic starting and the Curie temperatures. The ductility of these alloys is improved by the introduction of a small amount of the  $\gamma$ -phase. Consequently, the present new FSMAs are of great promise as smart materials.

<sup>1</sup>K. Ullakko, J. K. Huang, C. Kanter, V. V. Kokorin, and R. C. O'Handley, *Appl. Phys. Lett.* **69**, 1966 (1996).

<sup>2</sup>R. C. O'Handley, *J. Appl. Phys.* **83**, 3263 (1998).

<sup>3</sup>R. D. James and M. Wuttig, *Philos. Mag. A* **77**, 1273 (1998).

<sup>4</sup>T. Kakeshita, T. Takeuchi, T. Fukuda, T. Saburi, R. Oshima, S. Muto, and K. Kishio, *Mater. Trans., JIM* **41**, 882 (2000).

<sup>5</sup>F. Gejima, Y. Sutou, R. Kainuma, and K. Ishida, *Metall. Mater. Trans. A* **30**, 2721 (1999).

<sup>6</sup>A. Fujita, K. Fukamichi, F. Gejima, R. Kainuma, and K. Ishida, *Appl. Phys. Lett.* **77**, 3054 (2000).

<sup>7</sup>M. Wuttig, J. Li, and C. Craciunescu, *Scr. Mater.* **44**, 2393 (2001).

<sup>8</sup>K. Oikawa, L. Wulff, T. Iijima, F. Gejima, T. Ohmori, A. Fujita, K. Fukamichi, R. Kainuma, and K. Ishida, *Appl. Phys. Lett.* **79**, 3290 (2001).

<sup>9</sup>K. Oikawa, T. Ota, F. Gejima, T. Ohmori, R. Kainuma, and K. Ishida, *Mater. Trans.* **42**, 2472 (2001).

<sup>10</sup>Y. Murakami, D. Shindo, K. Oikawa, R. Kainuma, and K. Ishida, *Acta Mater.* **50**, 2173 (2002).

<sup>11</sup>H. Morito, A. Fujita, K. Fukamichi, R. Kainuma, K. Ishida, and K. Oikawa, *Appl. Phys. Lett.* **81**, 1657 (2002).

<sup>12</sup>T. B. Massalski, *Binary Alloy Phase Diagrams*, 2nd ed. (American Society for metals, metals Park, OH, 1990), pp. 1702 and 1832.

<sup>13</sup>R. Kainuma, H. Nakano, and K. Ishida, *Metall. Mater. Trans. A* **27A**, 4153 (1996).

<sup>14</sup>P. J. Webster, K. R. A. Ziebeck, S. L. Town, and M. S. Peak, *Philos. Mag. B* **49**, 295 (1984).

<sup>15</sup>K. Koho, J. Vimpari, L. Straka, O. Söderberg, O. Heczko, K. Ullakko, and V. K. Linderoos, *Abstracts International Conference on Martensitic Transformations ICOMAT 2002*, Helsinki, Finland, 2002, p. 296.